Adiabatic Shear Localization in Ultrafine Grained 6061 Aluminum Alloy

Article *in* Materials Science and Engineering A · September 2016

DOI: 10.1016/j.msea.2016.08.042

6 authors, including:

Bingfeng Wang
Central South University
39 PUBLICATIONS **71** CITATIONS
SEE PROFILE

Rui Ma
Central South University
4 PUBLICATIONS **1** CITATION
SEE PROFILE

Li Zezhou
University of California, San Diego
6 PUBLICATIONS **6** CITATIONS
SEE PROFILE

Shiteng Zhao
University of California, San Diego
18 PUBLICATIONS **26** CITATIONS
SEE PROFILE

Materials Science & Engineering A 675 (2016) 221–227

Contents lists available at ScienceDirect

Materials Science & Engineering A

journal homepage: www.elsevier.com/locate/msea

Adiabatic shear localization in ultrafine grained 6061 aluminum alloy

Bingfeng Wang [a,b,c,d,*], Rui Ma [a], Jindian Zhou [a], Zezhou Li [b], Shiteng Zhao [b], Xiaoxia Huang [a]

[a] School of Materials Science and Engineering, Central South University, Changsha 410083, People's Republic of China
[b] Department of Mechanical and Aerospace Engineering, University of California, San Diego, United States
[c] State Key Laboratory for Powder Metallurgy, Central South University, Changsha, Hunan, People's Republic of China
[d] Key Lab of Nonferrous Materials, Ministry of Education, Central South University, Changsha 410083, People's Republic of China

ARTICLE INFO

Article history:
Received 3 June 2016
Received in revised form
27 July 2016
Accepted 10 August 2016
Available online 20 August 2016

Keywords:
Electron microscopy
Aluminum alloys
Bulk deformation
Shear bands
Recrystallization

ABSTRACT

Localized shear is an important mode of deformation; it leads to catastrophic failure with low ductility, and occurs frequently during high strain-rate deformation. The hat-shaped specimen has been successfully used to generate shear bands under controlled shock-loading tests. The microstructure in the forced shear band was characterized by optical microscopy, microhardness, and transmission electron microscopy. The true flow stress in the shear region can reach 800 MPa where the strain is about 2.2. The whole shear localization process lasts for about 100 μs. The shear band is a long and straight band distinguished from the matrix by boundaries. It can be seen that the grains in the boundary of the shear band are highly elongated along the shear direction and form the elongated cell structures (0.2 μm in width), and the core of the shear band consists of a number of recrystallized equiaxed grains with 0.2 – 0.3 μm in diameters, and the second phase particles distribute in the boundary of the ultrafine equiaxed new grains. The calculated temperature in the shear band can reach about 667 K. Finally, the formation of the shear band in the ultrafine grained 6061 aluminum alloy and its microstructural evolution are proposed.

1. Introduction

Nowadays, grain refinement becomes one of the effective means to increase both the strength and plastic of the metallic material. Ultrafine grained 6061 aluminum alloy attracts tremendous interest in many industrial applications due to the excellent comprehensive properties, such as good coordination during the deformation, high strength, high toughness as well as resistance to deformation and impact. Recently, special attention has been paid to various ultrafine grained metallic materials with traditional compositions processed by severe plastic deformation process, such as high pressure torsion, accumulative roll-bonding, equal channel angular pressing, cyclic channel die compression, and friction stir processing [1–4]. Friction stir processing uses a rotating tool consisting of a threaded pin and tool shoulder to apply severe plastic deformation and frictional heating to the base metal to produce a strong metallurgical joint [5,6]. Among the various severe plastic deformation process available, friction stir processing is of great importance in many industrial applications and also is a new method to prepare bulk ultrafine grained materials due to its unique advantages, such as energy efficient, environment friendly, and versatile [7]. Many documented experimental and theoretical work have been focused on the microstructure and mechanical behavior of the ultrafine grained materials under quasi-static conditions [8]. However, the deformation characteristics of ultrafine grained 6061 aluminum alloy at the high-strain-rates and its mechanism are rarely reported, especially the adiabatic shear localization [9].

Adiabatic shear localization, or called adiabatic shear band, is a unique form of material failure under high strain rate loading commonly found in ballistic impact, explosive fragmentation, high-speed shaping and forming, dynamic compaction and welding, machining, and grinding. It is a signal of reduction or complete loss in deformation resistance of the material, and considered as an important precursor to material failure. Xu et al. [10] examined the microstructural aspects of adiabatic shear localization on different materials, such as low-carbon steel, stainless steel, titanium and its alloys, aluminum alloy and others. Owolabi et al. [11] investigated the dynamic impact response of cylindrical specimens of AA 2219-T8 alloy, and found that the transformed and deformed shear bands developed in the specimens, and the tendency to form adiabatic shear bands were influenced by the length to diameter ratio of the cylindrical test specimens. Zhu et al. [12] studied the melting phase transformation of aluminum alloy in the adiabatic shear band in the aluminum matrix composites. The

* Corresponding author at: School of Materials Science and Engineering, Central South University, Changsha 410083, People's Republic of China.
E-mail addresses: biw009@ucsd.edu, wangbingfeng@csu.edu.cn (B. Wang).

http://dx.doi.org/10.1016/j.msea.2016.08.042
0921-5093/

microstructure within shear bands in aluminum alloys observed in post-deformation observations provides some information to understand the thermal-mechanical evolution during the progress of shear localization. Depending on the materials and the experimental conditions employed, various mechanisms suggested for formation of the transformed bands include dynamic recrystallization [9,13–15], dynamic recovery [16] and phase transformation [17,18].

The aims of this paper are (1) to obtain the mechanical response of ultrafine grained 6061 aluminum alloy processed by friction stir processing under controlled dynamic conditions, and (2) to characterize the microstructure in a shear band, and (3) to propose the microstructural mechanism of the shear band.

2. Experimental and procedures

The material used in this study is ultrafine grained 6061 aluminum alloy with the grain size about 1 μm processed by the friction stir deformation (Fig. 1). Friction stir deformation process is schematically shown in Fig. 2. The processing parameters include: 80 mm/min traveling speed, 1000 rpm clockwise rotating speed, using a tool with 26 mm shoulder diameter and 10 mm pin diameter with 12.5 mm pin depth for full penetration into the plates.

The hat-shaped specimens, originally designed by Meyer and Manwaring [19], were used to force an adiabatic shear band to form in a narrow zone. It was used to produce a shear band in the ultrafine grained 6061 aluminum alloy at high strain rate under controlled dynamic compression conditions using a split Hopkinson pressure bar at 293 K. The sizes of the hat shaped specimens are shown in Fig. 3. By setting the control loop with different thickness, the shear deformation with different nominal shear strains were prepared on the hat-shaped specimens.

The samples for investigation were cut from the hat-shaped specimens by electrical discharge machining. The sectioned surfaces were polished and etched by 3 ml nitric acid +6 ml hydrofluoric acid +6 ml hydrochloric acid +150 ml H_2O (Keller reagent). Optical microscope was performed with POLYVAR-MET.

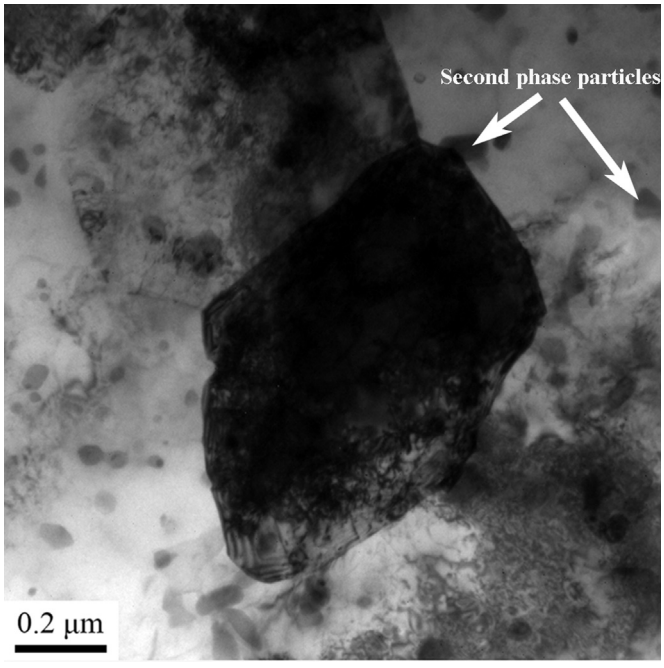

Fig. 1. Initial microstructure of the specimens.

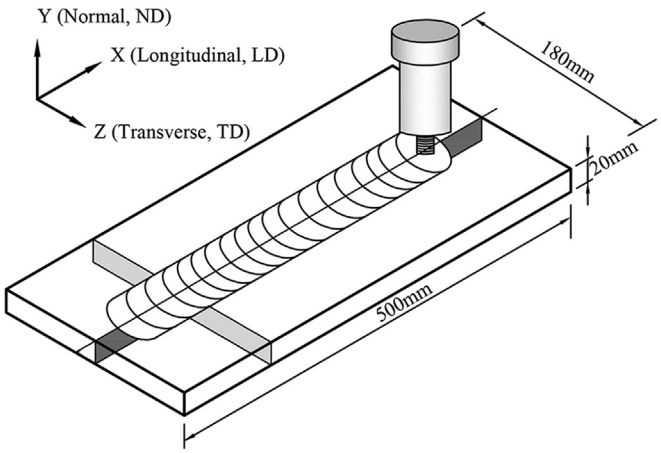

Fig. 2. Schematic diagram of the friction stir process (FSP).

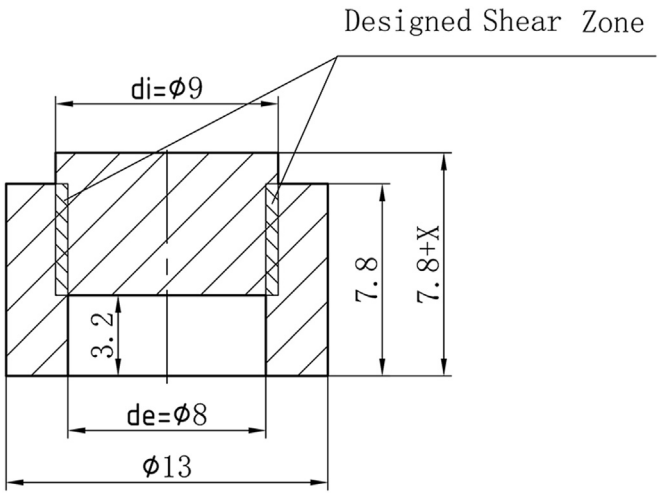

Fig. 3. Schematic diagram of the hat-shaped specimen (Dimensions in mm).

Microhardness tests were performed with HMV-2T. The loading mass is 0.025 kg, and the loading time is 10 s. Transmission electron microscopy (TEM) samples were obtained by polishing samples to thin foils. Then the foils were perforated upon the shear band (Fig. 4) by electro-polishing in solution of 30 ml nitric acid +70 ml Methanol at 243 K. TEM observations were carried out

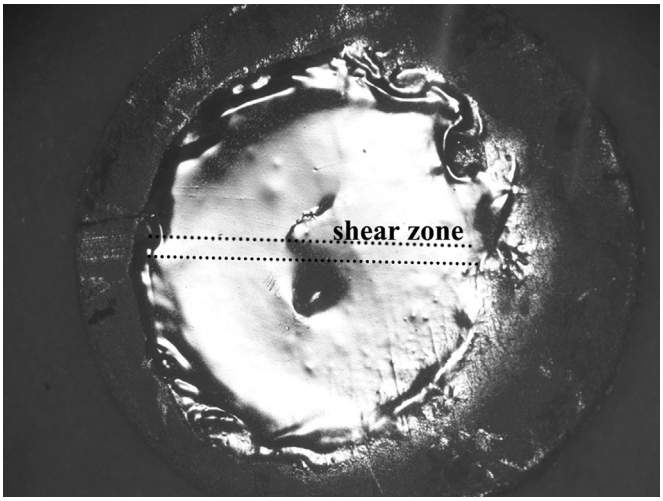

Fig. 4. Low-magnification optical microscope image of the TEM disk. The black dot line is along the shear zone.

with a Tecnai G^2 20 transmission electron microscope operated at 200 kV.

3. Results and discussion

3.1. Mechanical response of the specimen

When the specimen was compressed by a split Hopkinson pressure bar, the force applied to the shear band was calculated from data collected by the strain gauges on the incident and transmitted bars. The shear stress, strain rate, nominal strain and the true tress can be calculated by the following equations [20,21].

$$\tau = \frac{E_0 A_s \varepsilon_t(t)}{\pi h(\frac{d_i + d_e}{2})} \quad (1)$$

$$\dot{\gamma} = \frac{2C_0\left[(\varepsilon_i(t) - \varepsilon_t(t)\right]}{s} \quad (2)$$

$$\gamma = \frac{2C_0 \int_0^t \left[(\varepsilon_i(t) - \varepsilon_t(t)\right]dt}{s} \quad (3)$$

$$\sigma = 2\tau \quad (4)$$

where E_0 and C_0 are the elastic modulus and the elastic wave speed in the split Hopkinson pressure bar (E_0=200 GPa, C_0=5000 m/s); A_s is the cross section area of the bar; h and s are the length and the width of the shear band (s is measured on the section plane using a metalloscope); d_i and d_e are the geometrical parameters of the hat-shaped specimen shown in Fig. 3; and $\varepsilon_i(t)$ and $\varepsilon_t(t)$ are the experimentally measured strain using incident and transmitted stress pulse on the split Hopkinson pressure bars, respectively.

Culver [22] introduced a simple relation between the true strain and the shear strain expressed as Eq. (5).

$$\varepsilon = \ln\sqrt{1 + \gamma + \frac{\gamma^2}{2}} \quad (5)$$

Experimentally measured voltage pulse on the ultrafine grained 6061 aluminum alloy specimen is shown in Fig. 5(a). The average strain rate during shear deformation can be calculated from Fig. 5(b) and Eq. (2), and is about $1.2 \times 10^5\ s^{-1}$, which is extremely high in comparison with $1 \times 10^{-1}\ s^{-1}$ during quasi-static deformation. The forced shearing deformation starts from the first peak value of the strain rate to the last loading stress peak [20]. The time for the forced shear localization is about 100 μs. The relationship of the true stress and the true strain shown in Fig. 5 (c) can be calculated from Eqs. (1) to (5). There are three stages proceeded during the dynamic loading. In the first stage (a-b), the true flow stress increases with the true strain due to the strain hardening and strain rate hardening, and the true flow stress reaches about 440 MPa. In the second stage (b-c), the true flow stress increases progressiveely as a result of the balance of the thermal softening, strain hardening and strain rate hardening. The true flow stress reaches the maximum value of 800 MPa where the strain is about 2.2. In the third stage (c-d), the true stress sharply decreases with increasing the strain at point c. Thermal softening dominated the deformation process beyond the peak stress leading to fall in stress with increase in strain. This signals the onset of mechanical instabilities that result in strain localization and adiabatic shear bands. Overall, plastic deformation in metallic

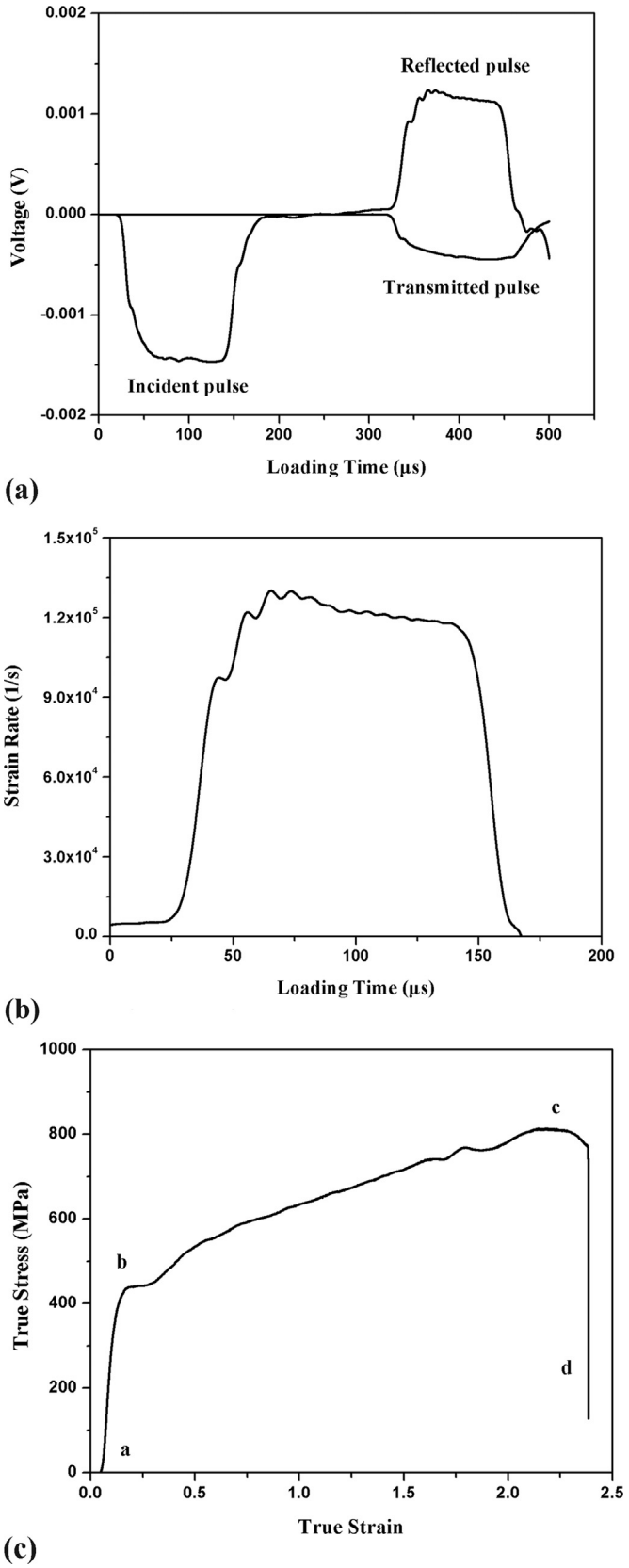

Fig. 5. Dynamic responses of ultrafine grained 6061 aluminum alloy specimen at high strain rate. (a) Shear signals with the hat shaped specimen attached between the bars; (b) strain rate-time curves; (c) true stress–true strain curves.

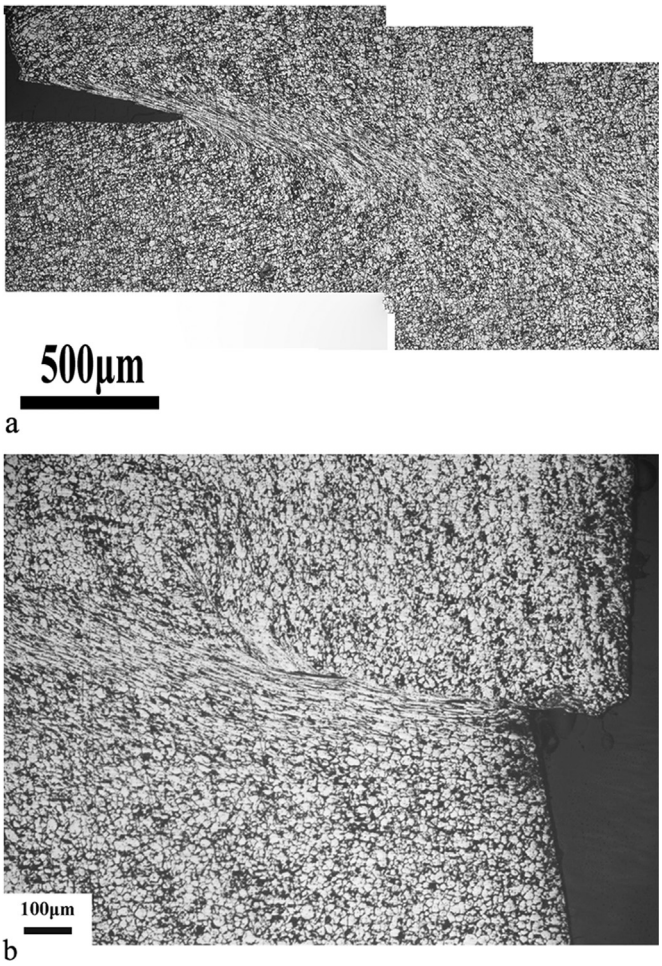

Fig. 6. Optical micrographs of the shear band produced in the specimen. (a) a shear band; (b) part of the shear band.

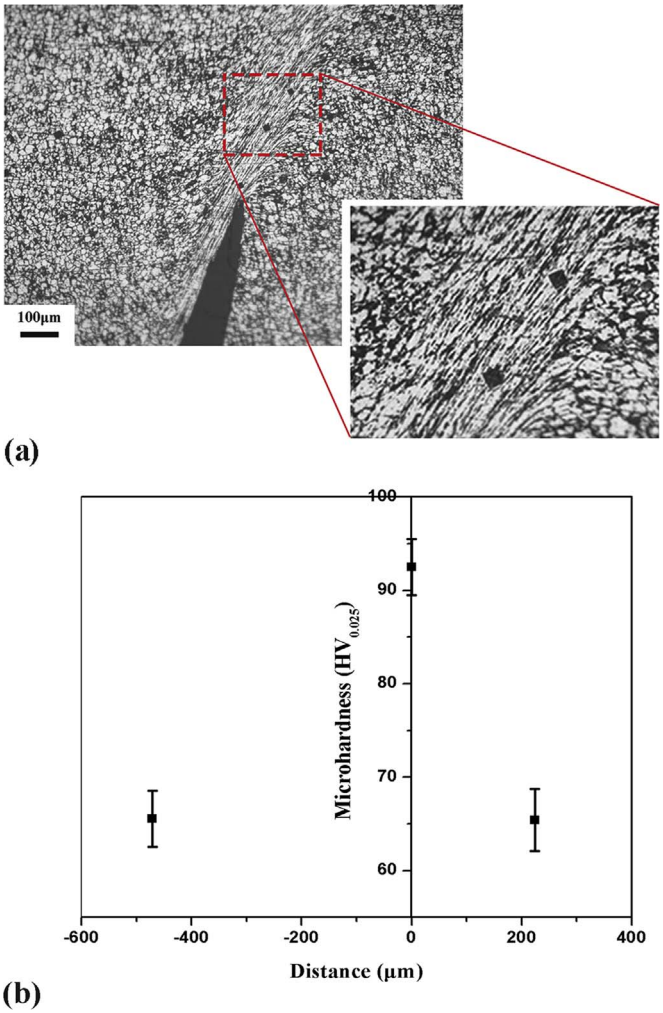

Fig. 7. (a) Optical micrograph of microhardness testing zone; (b) Microhardness distribution across the shear band in the ultrafine grained specimen.

materials under dynamic impact loading is a complex phenomenon that is characterized by competing strain hardening effect of dislocation multiplication during plastic deformation and thermal softening effect of conversion of impact energy to thermal energy leading to temperature increase in the impacted alloy.

3.2. Microstructure within the forced shear region

Fig. 6 shows the optical micrographs of the shear sections in the ultrafine grained aluminum alloys. It can be seen that the shear band is a long and straight band distinguished from the matrix by boundaries. The width of the shear band is about 100 μm.

Fig. 7 shows the microhardness of a shear band in ultrafine grained 6061 aluminum alloy. It can be found that microhardness within the shear band is much higher than that in the matrix.

Fig. 8(a) and (b) show the grains in the boundary of the shear band. It can be seen that these grains are highly elongated along the shear direction and form the elongated cell structures (0.2 μm in width) due to the shear deformation upon the shear band; elongated cell structures break up into several subgrains; the second phase particles are distributed on the grain boundaries. The center of the shear band consists of a number of equiaxed grains 0.2 – 0.3 μm in diameters (Fig. 8(c) and (d)) with low dislocations density. These ultrafine equiaxed grains have well defined boundaries and typical recrystallization features. It is also found that the second phase particles exist in the boundary of the equiaxed new grains. These second phase particles precipitated at the grain boundaries of the recrystallization grains play a role in pinning the grain boundaries and strengthening the materials.

3.3. Microstructure mechanism in the shear zone

At high strain rates ($> 1 \times 10^3\ s^{-1}$), the deformation process is extremely fast and can be considered as an adiabatic process. Temperature rise in the adiabatic shear band associated with the deformation plays a significant role in the study of microstructure mechanism and is calculated by the following equation [9,14].

$$\Delta T = T - T_0 = \frac{\eta_T}{\rho C_V} \int_{\varepsilon_s}^{\varepsilon_e} \sigma d\varepsilon \tag{6}$$

where T_0 is the ambient temperature, and η_T is the fraction of plastic energy converted to heat, commonly $\eta_T = 0.9$. For 6061 aluminum alloy [23], $\rho = 2700\ kg/m^3$, $C_v = 0.88 \times 10^3\ J/(kg \cdot K)$, $T_0 = 298\ K$.

The flow stress–strain response of the 6061-T6 aluminum alloy specimens can be adequately described by the Zerilli–Armstrong model for face centered cubic structure [24].

$$\sigma = C_0 + C_2 \varepsilon^n [e^{(-C_3 T + C_4 T \ln \dot{\varepsilon})}] \tag{7}$$

where C_0, C_2, n, C_3 and C_4 are constants. Note that $C_0 = \sigma_G + PD^{-1/2}$, where σ_G is related to microstructural effects and $PD^{-1/2}$ is the Hall–Petch grain size term, in which P is the Petch constant and D

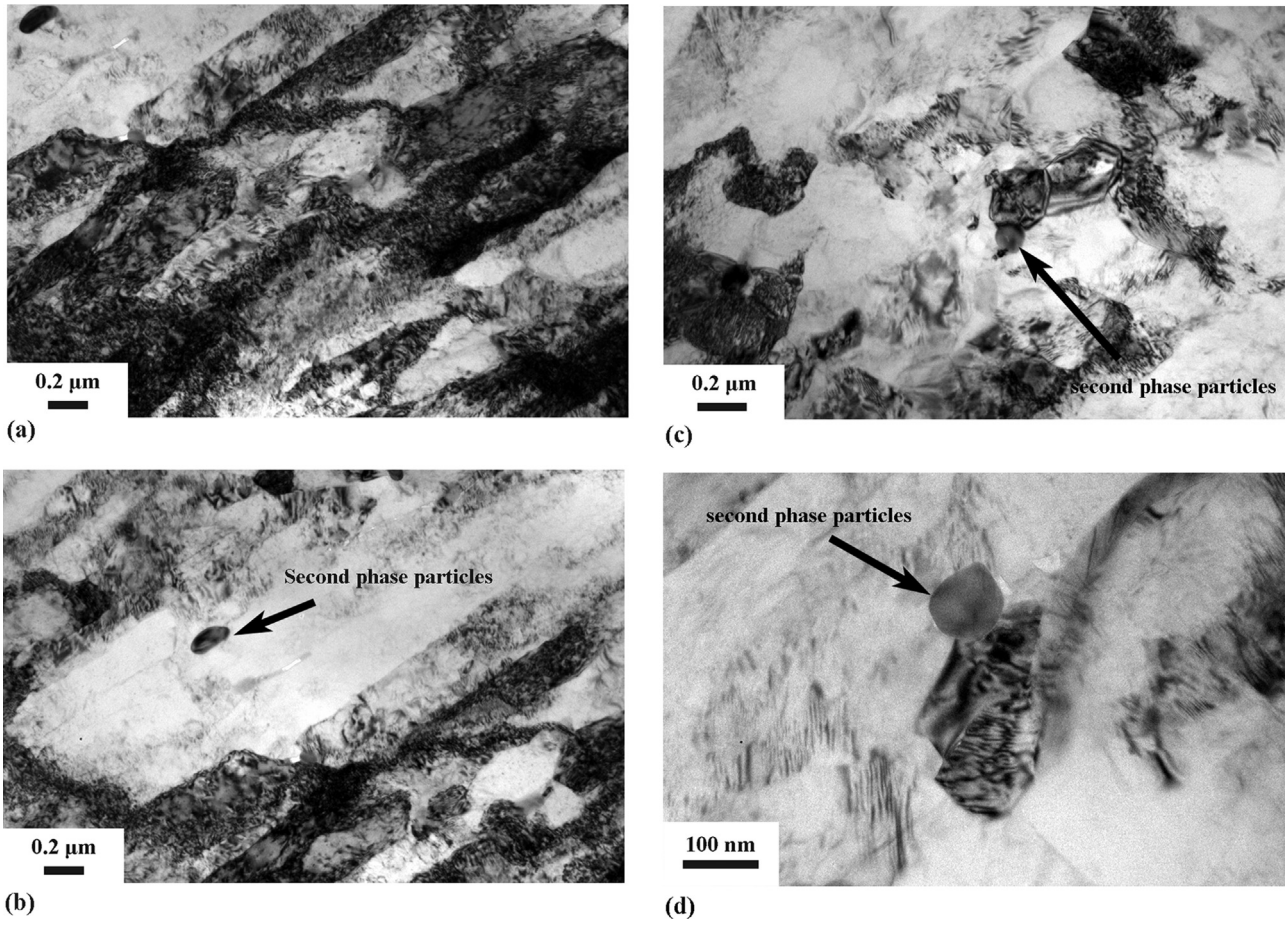

Fig. 8. Bright field patterns of the microstructure in the shear band in the ultrafine grained specimen. (a) and (b) the microstructure in the boundary of the shear band; (c) and (d) the microstructure in the core of the shear band.

is the grain size. Furthermore, σ is the stress, ε is the equivalent plastic strain, $\dot{\varepsilon}$ is the strain rate, and T is the deformation temperature. The constants in the Zerilli–Armstrong model for the 6061-T6 aluminum alloy were found to be as follows, σ_G=150.82 MPa; P =83.79 MPa $\mu m^{1/2}$; n =0.0624; C_2=710.40 MPa; $C_3=5.5\times10^{-3}(K^{-1})$ and $C_4=4.4\times10^{-4}(K^{-1})$ [24].

It can be calculated that the maximum temperature in the forced localized shear zone is about 667 K. The recrystallization temperature of 6061 aluminum alloy can be taken as 0.4 – 0.6 T_m (350 – 523 K). Therefore, the temperature rise in a shear band meets the needs of the recrystallization of 6061 aluminum alloy.

The microstructures of the shear band in the ultrafine grained 6061 aluminum alloy processed by friction stir processing indicate that the ultrafine equiaxed grains are formed in the core of the shear band, and the second phase particles were distributed in the boundary of the ultrafine equiaxed new grains. The thermodynamic calculation results suggest that the dynamic recrystallization mechanism may take effect on the ultrafine grained 6061 aluminum alloy.

Recrystallization arising from high-strain-rate loading has been well documented by some materials scientists in decades. The investigations have indicated many models to explain the dynamic recrystallization in the adiabatic shear band. According to the rotational dynamic recrystallization mechanism[9,14], formation of a new grain requires that local grain-boundary segments can tilt about 30° within the deformation process [14]. The time needed for these processes can be expressed as follows [14].

$$t = \frac{L_1 kTf(\theta)}{4\delta\eta D_{b0}\exp(-Q_b/RT)} \tag{8}$$

where t is time; L_1 is the average subgrains diameter; δ is grain-boundary thickness; η is the grain boundary energy; D_{b0} is a constant related to grain boundary diffusion; Q_b denotes the activation energy for grain boundary diffusion. θ is the subgrains misorientation, and f(θ) can be described as follow.

$$f(\theta) = \frac{3\tan(\theta) - 2\cos(\theta)}{3 - 6\sin(\theta)} + \frac{2}{3} - \frac{4\sqrt{3}}{9} ln\frac{2+\sqrt{3}}{2-\sqrt{3}} + \frac{4\sqrt{3}}{9} ln\frac{\tan(\theta/2) - 2 - \sqrt{3}}{\tan(\theta/2) - 2 + \sqrt{3}} \tag{9}$$

For aluminum alloy, $\delta D_{b0}=9.9\times10^{-14}$ m^3/s, η=0.324 J/m^2, Q_b=100 kJ/mol, k $=1.38\times10^{-23}$ J/K, R =8.314 J/(K • mol) [25]. For specimen c-1 ($\gamma_{nominal}$=2.6), the maximum temperature within the shear band is calculated about 667 K (0.75 T_m) and the whole time for the dynamic loading lasts for 40 μs. The kinetic curve for the rotational dynamic recrystallization mechanism in the shear band can be obtained by integrating the parameters into Eqs. (8) - (9), as shown in Fig. 9. The temperature varies from 0.65 T_m to 0.75 T_m for a subgrain size of 200 nm (Fig. 9(a)), and the subgrain size L_1 is varied from 200 nm to 500 nm at T =0.75T_m (667 K) (Fig. 9(b)). Smaller subgrains and higher temperature result in the recrystallization much sooner. The results show that the grain-boundary rotation is accomplished within 12 μs when the subgrain size L_1 varies from 200 nm to 500 nm at T =0.75 T_m (667 K). It is worth noting that the deformation time (100 μs) is

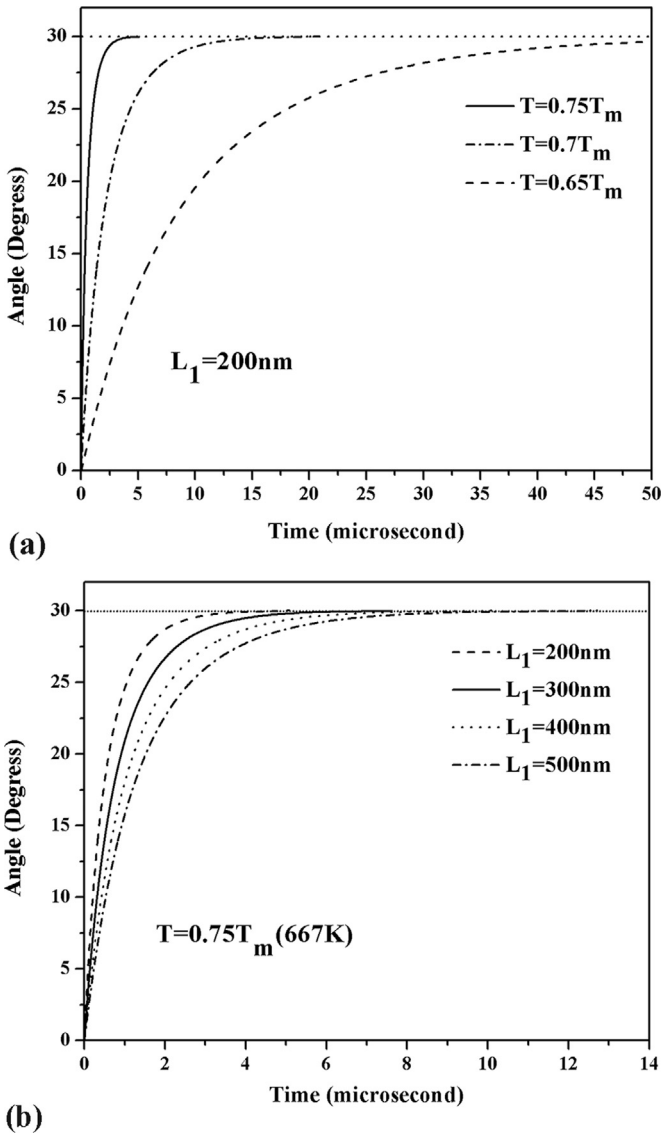

Fig. 9. Angle of rotation of subgrains boundary in the shear band in the ultrafine grained specimen as a function of needed time for (a) different temperatures for $L_1=200$ (nm) ; (b) different subgrains size at 0.75 T_m (667 K).

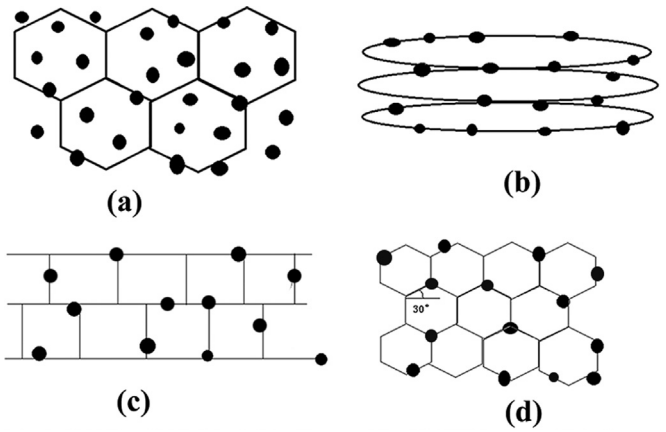

Fig. 10. Schematic diagram illustrates the microstructural evolution within the shear band in the ultrafine grained 6061 aluminum alloy.

enough for the formation of the ultrafine grains in the shear band by way of the subgrains boundaries rotation. Thus, the rotational dynamic recrystallization mechanism can take effect on the formation of the new equiaxed grains in ultrafine grained 6061 aluminum alloy.

Therefore, the microstructural evolution in the adiabatic shear band in the ultrafine grained 6061 aluminum alloy can be described as follows (Fig. 10). The second phase particles are distributed randomly in the original state (a); At the beginning of the shear deformation, the dislocations in the shear deformation region are immediately accumulated to form elongated cells along the shear direction, and the second phase particles are mainly distributed along the grain boundaries (b); With the reducing of the width of cell structure, the elongated dislocation cells break up, resulting in the formation of approximately equiaxed subgrains, and the second phase particles can be found at the grain boundaries because the size of the second phase particles and the equiaxed grains are basically the same (c); Then, the grain boundaries of the equiaxed subgrains rotate about 30°and form the nanosized equiaxed grains with high-angle grain boundaries, and the second phase particles are pinning at the boundaries of the equiaxed grains (d). The rotational grain boundaries cannot grow significantly after deformation because of the fast cooling rate in the shear band and the lack of mechanical assistance during the cooling stage [26].

4. Conclusions

Shear localization in ultrafine grained 6061 aluminum alloy processed by friction stir processing under controlled dynamic conditions was characterized in this paper. Unstable shear deformation of the alloy emerges after the true flow stress reaches about 440 MPa, and the true flow stress in the shear region increases sharply and reaches the maximum value of 800 MPa. The whole shear localization process lasts about 100 μs. The adiabatic shear band in ultrafine grained 6061 aluminum alloy is a long and straight band distinguished from the matrix by boundaries. The grains in the boundary of the shear band are highly elongated along the shear band, forming the elongated cell structures (0.2 μm in width), and the core of the band consists of a number of equiaxed grains 0.2 – 0.3 μm in diameters. The second phase particles do not disappear, and exist in the boundary of the new grains in the core of the shear band. The calculated temperature in the shear band is estimated to reach 667 K which meets the needs of recrystallization of aluminum alloy. Rotational dynamic recrystallization takes effect on the formation of microstructure in the adiabatic shear band of the ultrafine grained 6061 aluminum alloy.

Acknowledgments

This work was financial supported by Hunan Provincial Natural Science Foundation of China (No. 12JJ2028), and by the Freedom Explore Program of Central South University (No. 2015zzts175), and by State Key Laboratory of Powder Metallurgy, Central South University, China. The authors would like to express their sincere thanks to Professor M. A. Meyers and K. S. Vecchio at university of California, San Diego for good suggestions and helps.

References

[1] N.X. Zhang, N.Q. Chinh, M. Kawasaki, Y. Huang, T.G. Langdon, Self-annealing in a two-phase Pb-Sn alloy after processing by high-pressure torsion, Mater. Sci.

Eng. A 666 (2016) 350–359.
[2] A.P. Zhilyaev, T.G. Langdon, Using high-pressure torsion for metal processing: Fundamentals and applications, Prog. Mater. Sci. 53 (2008) 893–979.
[3] N. Sridharan, M. Gussev, R. Seibert, C. Parish, M. Norfolk, K. Terrani, S.S. Babu, Rationalization of anisotropic mechanical properties of Al-6061 fabricated using ultrasonic additive manufacturing, Acta Mater. 117 (2016) 228–237.
[4] M.M. Mahdavian, L. Ghalandari, M. Reihanian, Accumulative roll bonding of multilayered Cu/Zn/Al: An evaluation of microstructure and mechanical properties, Mater. Sci. Eng. A 579 (2013) 99–107.
[5] S. Malopheyev, S. Mironov, I. Vysotskiy, R. Kaibyshev, Superplasticity of friction-stir welded Al–Mg–Sc sheets with ultrafine-grained microstructure, Mater. Sci. Eng. A 649 (2016) 85–92.
[6] X.C. He, F.S. Gu, Andrew Ball, A review of numerical analysis of friction stir welding, Prog. Mater. Sci. 65 (2014) 1–66.
[7] Z.Y. Ma, R.S. Mishra, M.W. Mahoney, Superplastic deformation behaviour of friction stir processed 7075Al alloy, Acta Mater. 50 (2002) 4419–4430.
[8] J. An, Y.F. Wang, Q.Y. Wang, W.Q. Cao, C.X. Huang, The effects of reducing specimen thickness on mechanical behavior of cryo-rolled ultrafine-grained copper, Mater. Sci. Eng. A 651 (2016) 1–7.
[9] B. Dodd, Y.L. Bai, Adiabatic Shear Localization: Frontiers and Advances, second ed, Elsevier Science Ltd,, London, 2012.
[10] Y. Xu, J. Zhang, Y. Bai, M.A. Meyers, Shear Localization in Dynamic Deformation: Microstructural Evolution, Metall. Mater. Trans. A 39 (2008) 811–843.
[11] G.M. Owolabi, D.T. Bolling, A.A. Tiamiyu, R. Abu, A.G. Odeshi, H.A. Whitworth, Shear strain localization in AA 2219-T8 aluminum alloy at high strain rates, Mater. Sci. Eng. A 655 (2016) 212–220.
[12] D. Zhu, Z. Zheng, Q. Chen, Adiabatic shear failure of aluminum matrix composites and microstructural characteristics of transformed bands, Mater. Sci. Eng. A 595 (2014) 241–246.
[13] Y. Jiang, Z. Chen, C. Zhan, T. Chen, R. Wang, C. Liu, Adiabatic shear localization in pure titanium deformed by dynamic loading: Microstructure and microtexture characteristic, Metall. Mater. Sci. Eng. A 640 (2015) 436–442.
[14] M.A. Meyers, Y.B. Xu, Q. Xue, M.T. Perez-Prado, T.R. McNelley, Microstructural evolution in adiabatic shear localization in stainless steel, Acta Mater. 51 (2003) 1307–1325.
[15] A.A. Tiamiyu, Ritwik Basu, A.G. Odeshi, Jerzy A. Szpunar, Plastic deformation in relation to microstructure and texture evolution in AA 2017-T451 and AA 2624-T351 aluminum alloys under dynamic impact loading, Mater. Sci. Eng. A 636 (2015) 379–388.
[16] M.T. Pérez-Prado, J.A. Hines, K.S. Vecchio, Microstructural evolution in adiabatic shear bands in Ta and Ta–W alloys, Acta Mater. 49 (2001) 2905–2917.
[17] B.F. Wang, J. Sun, X. Wang, A. Fu, Adiabatic shear localization in a near beta Ti–5Al–5Mo–5 V–1Cr–1Fe alloy, Mater. Sci. Eng. A 639 (2015) 526–533.
[18] L.E. Murr, A.C. Ramirez, S.M. Gaytan, M.I. Lopez, E.Y. Martinez, D.H. Hernandez, E. Martinez, Microstructure evolution associated with adiabatic shear bands and shear band failure in ballistic plug formation in Ti–6Al–4V targets, Mater. Sci. Eng. A 516 (2009) 205–216.
[19] L.W. Meyer, S. Manwaring, in: L.E. Murr, K.P. Staudhammer, M.A. Meyers (Eds.), Metallurgical Applications of Shock-Wave and High-Strain-Rate Phenomena, Marcel Dekker, New York, 1986, pp. 657–674.
[20] U. Andrade, M.A. Meyers, K.S. Vecchio, A.H. Chokshi, Dynamic recrystallization in high-strain, high-strain-rate plastic deformation of copper, Acta Metall. Mater. 42 (1994) 3183–3195.
[21] Q. Li, Y.B. Xu, Z.H. Lai, L.T. Shen, Y.L. Bai, Dynamic recrystallization induced by plastic deformation at high strain rate in a Monel alloy, Mater. Sci. Eng. A276 (2000) 250–256.
[22] R.S. Culver, Metallurgical Effects at High Strain Rates, in: R.W. Rohde, B. M. Butcher, J.R. Holland (Eds.), Plenum Press, New York, 1973, pp. 519–523.
[23] D.H. Li, Y. Yang, T. Xu, H.G. Zheng, Q.S. Zhu, Q.M. Zhang, Observation of the microstructure in the adiabatic shear band of 7075 aluminum alloy, Mater. Sci. Eng. A527 (2010) 3529–3535.
[24] W.S. Lee, Z.C. Tang, Relationship between mechanical properties and microstructural response of 6061-T6 aluminum alloy impacted at elevated temperatures, Mater. Des. 58 (2014) 116–124.
[25] N. Du, A.F. Bower, P.E. Krajewski, Numerical simulations of void growth in aluminum alloy AA5083 during elevated temperature deformation, Mater. Sci. Eng. A 527 (2010) 4837–4846.
[26] B.F. Wang, J.Y. Sun, E.N. Hahn, X.Y. Wang, Shear Localization and its Related Microstructure Mechanism in a Fine-Grain-Sized Near-Beta Ti Alloy, J. Mater. Eng. Perform. 24 (2015) 477–483.